AD-A039 796 NORTHROP CORP ROLLING MEADOWS ILL DEFENSE SYSTEMS DIV F/G 9/5
LOW COST EXPENDABLE TWT AMPLIFIER FOR ECM.(U)
APR 77 N00173-76-C-0305
UNCLASSIFIED NL

1 OF 1
ADA039 796

END
DATE
FILMED
6-77

AD A 039796

NORTHROP

Northrop Corporation   Defense Systems Div[redacted]

600 Hicks Road
Rolling Meadows, Illinois 60008

Telephone: 312/259-9600
TWX: 910/687-3785

D NW

11

7 Apr[redacted]77

12 28p.

Contracting Officer
Naval Research Lab.
Washington, D.C. 20375

Attention: Mrs. M. Corley/Code 2415.MC

Subject: Contract (15) N00173-76-C-0305 new
2nd Quarterly Report. no. 2, 26 Nov 76-28 Feb 77

Our Reference: (9) E.P. 8533 Progress
DES-77-454

Gentlemen:

Be advised that in accordance with subject contract line Item 0002 requirements, the required copies of Quarterly Report A001 covering period 26 November 1976 thru 28 February 1977 have been distributed to the addresses on the attached list.

Very truly yours,

Donita Shaw
Contract Administrator

/km

cc: DCASMA-Chicago/A. Sears/DCRI-GCCB-BF
DCASMA-Chicago/W. Tolar/DCRI-GCPB

(6) Low Cost Expendable TWT Amplifier for ECM.

S/C 409 213

	DODAAD Code	Number of Copies Unclass.
Teledyne MEC Palo Alto, Calif. 94304 Attention: Dr. N. Pond	11312	1
ITT Electron Tube Division Easton, Pennsylvania 18042 Attention: Mr. Workman	20948	1
Varian Associates Tube Div. Palo Alto, Calif. 94304 Attention: Mr. W. Luebke	6E845	1
Litton Industries Electron Tube Division San Carlos, Calif. 94070 Attention: Mr. S. Weber	80080	1
Raytheon Power Tube Div. Foundry Avenue Waltham, Mass. 02054 Attention: Mr. L. Clampett	6H339	1
Hughes Aircraft Company Electron Dynamics Division Lomita Boulevard Torrance, Calif. 90509 Attention: Mr. A. Lavik	73293	1
Director Naval Electronics Laboratory Center San Diego, Calif. 92152 Attention: Code 3260	N00953	1
Director Rome Air Development Center Griffiss AFB, New York 13441 Attention: Mr. D. Bussey	FY7619	1
Microwave Associates, Inc. Burlington, Mass. 01803 Attention: Mr. J. Brown, EW Components		1
Advisory Group on Electron Devices 201 Varick Street New York, New York 10014 Attention: Mr. H. R. Summer		1

In the event that information to be included in the above reports is proprietary to the contractor, this information may be removed from the main reports and delivered as appendices separately only to the governmental agencies of the distribution list.

	DODAAD Code	Number of Copies Unclass
Director, Naval Research Laboratory Washington, D.C. 20375	N00173	
Attention: Codes 5733 (Durkin)		1
5700		1
5740		1
5750		1
5706		1
5709		3
5230 (Haas)		1
Director, Naval Electronic Systems Command National Center #1 Arlington, Virginia 20360	N00039	
Attention: Code 304 (Butler)		3
Director, Naval Air Systems Command Jefferson Plaza Washington, D.C. 20361	N00019	
Attention: AIR 53322D (Whiting)		3
Defense Documentation Center Building 5, Cameron Station	S47031	
Alexandria, Virginia 22314		12
Naval Weapons Center China Lake, California 93555	N60530	
Attention: Code 3544 (Scott)		1
Director, Naval Electronic Systems Command National Center #1 Arlington, Virginia 20360	N00039	
Attention: PME-107-5		3
Director, Naval Electronic Systems Command National Center #1 Arlington, Virginia 20360	N00039	
Attention: Code 350		2
Watkins-Johnson Company 3333 Hillview Avenue Palo Alto, California 94304	14482	
Attention: Mr. G. Wada		1

LOW COST EXPENDABLE TWT AMPLIFIER FOR ECM

CONTRACT NO. N00173-76-C-0305

2ND QUARTERLY PROGRESS REPORT

26 NOVEMBER 1976 - 28 FEBRUARY 1977

1. ACCOMPLISHMENTS

1.1 Tolerances

The influences of the angle between the beam forming electrode and the cathode was computed. Figure 1 shows the general structure of the gun and Table 1 the results.

TABLE 1

Angle	μ Perveance	Max. current density / Min. current density	Beam interception
40^{o}	.39	1.34	0
45^{o}	.46	1.06	0
50^{o}	.55	1.22	0
55^{o}	.62	1.40	20%

For a perveance of .46 μP ± 5% the angle must be constant at $45^{o} \pm 1.5^{o}$.

1.2 Perveance

In the first trimestrial reports a large discrepancy between the calculated and measured perveances was found. Several guns with the same dimensions were tested. Table 2 shows the experimental results:

TABLE 2

	1	2	3	4	.5	Computed
Perveance	41	44	.39-.50	.45	.46	.46

Note that Gun No. 3 had a Medicus cathode.

Two different characterisitcs of degradation by poisoning were observed. Figure 2 shows the normal $I^{2/3}$-V characteristic before and after poisoning. Figure 3 shows the characteristic of Gun No. 1. Even up to 3.5 kV the cathode was space charge limited, however the perveance was low. This can only be explained by assuming that one part of the cathode was non-emitting.

It can be considered that the SAI program for the gun calculation is in good agreement with experience. The discrepancy described in the first trimestrial report is due to poor technology.

1.3 Medicus Cathode.

Considerable difficulty was encountered with the poisoning of the impregnated cathode. The vacuum station was several times modified

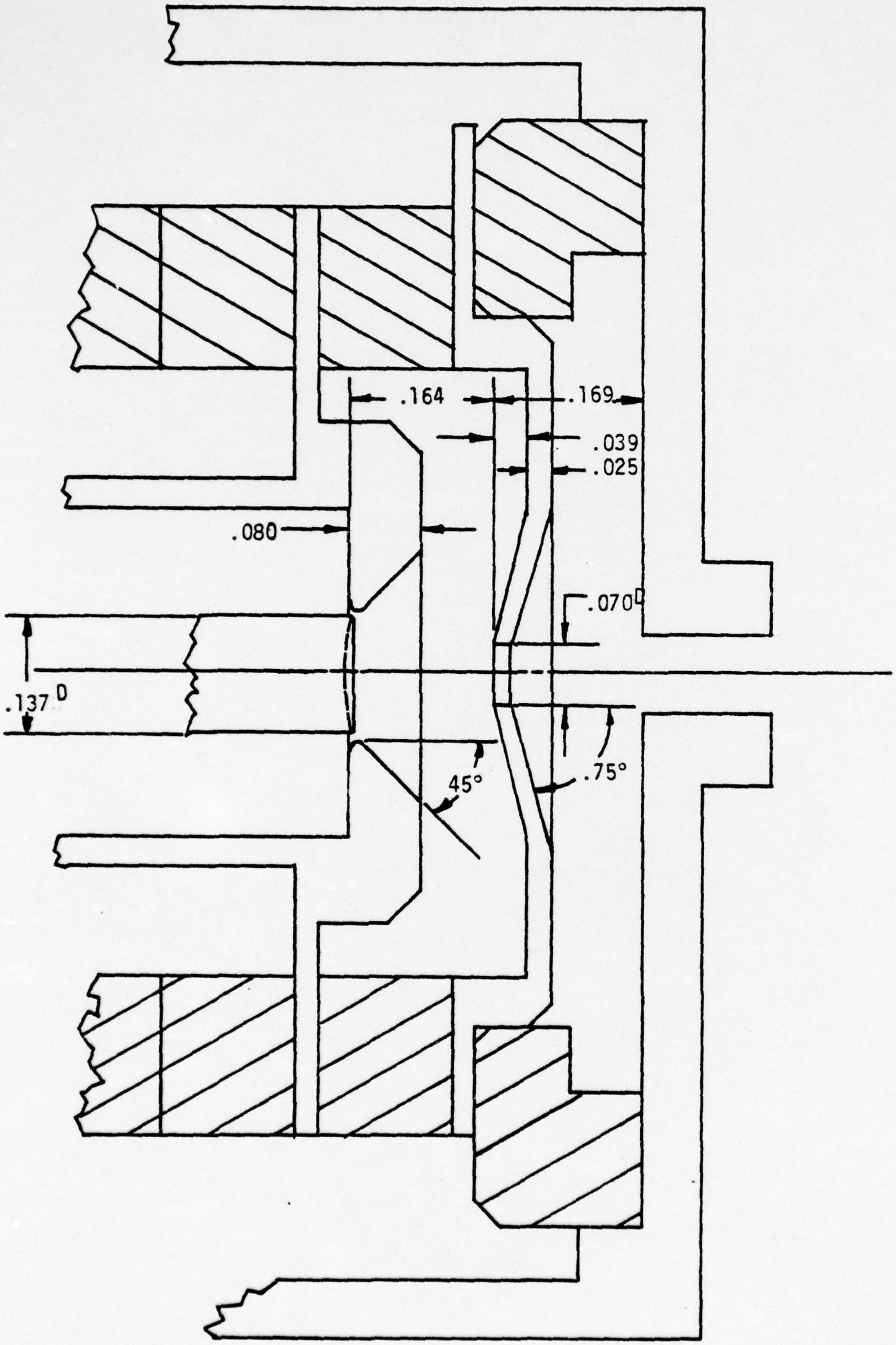

FIGURE 1: CROSS SECTION OF ELECTRON GUN

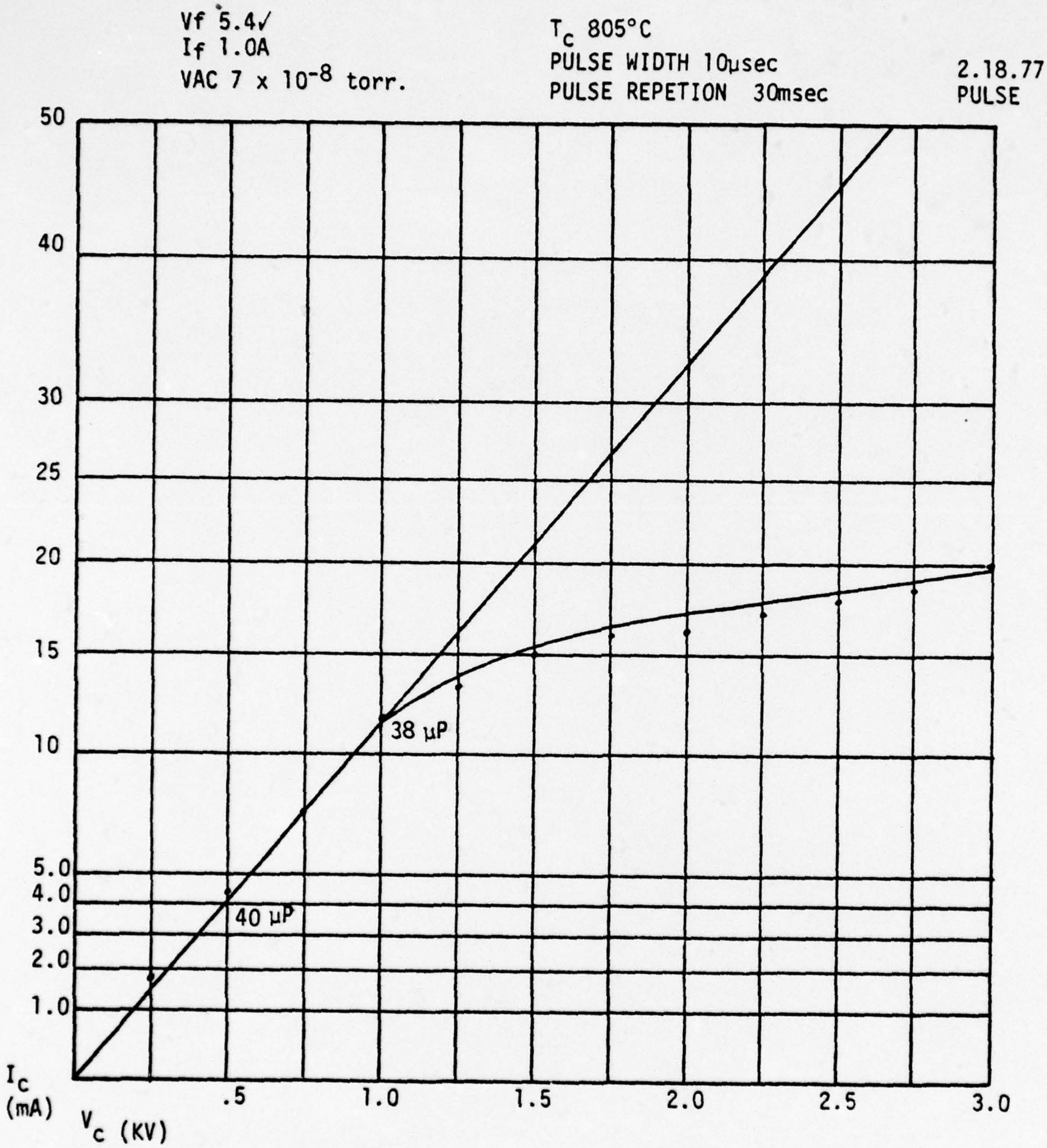

FIGURE 2: TWT BEAM TESTER CHARACTERISTIC

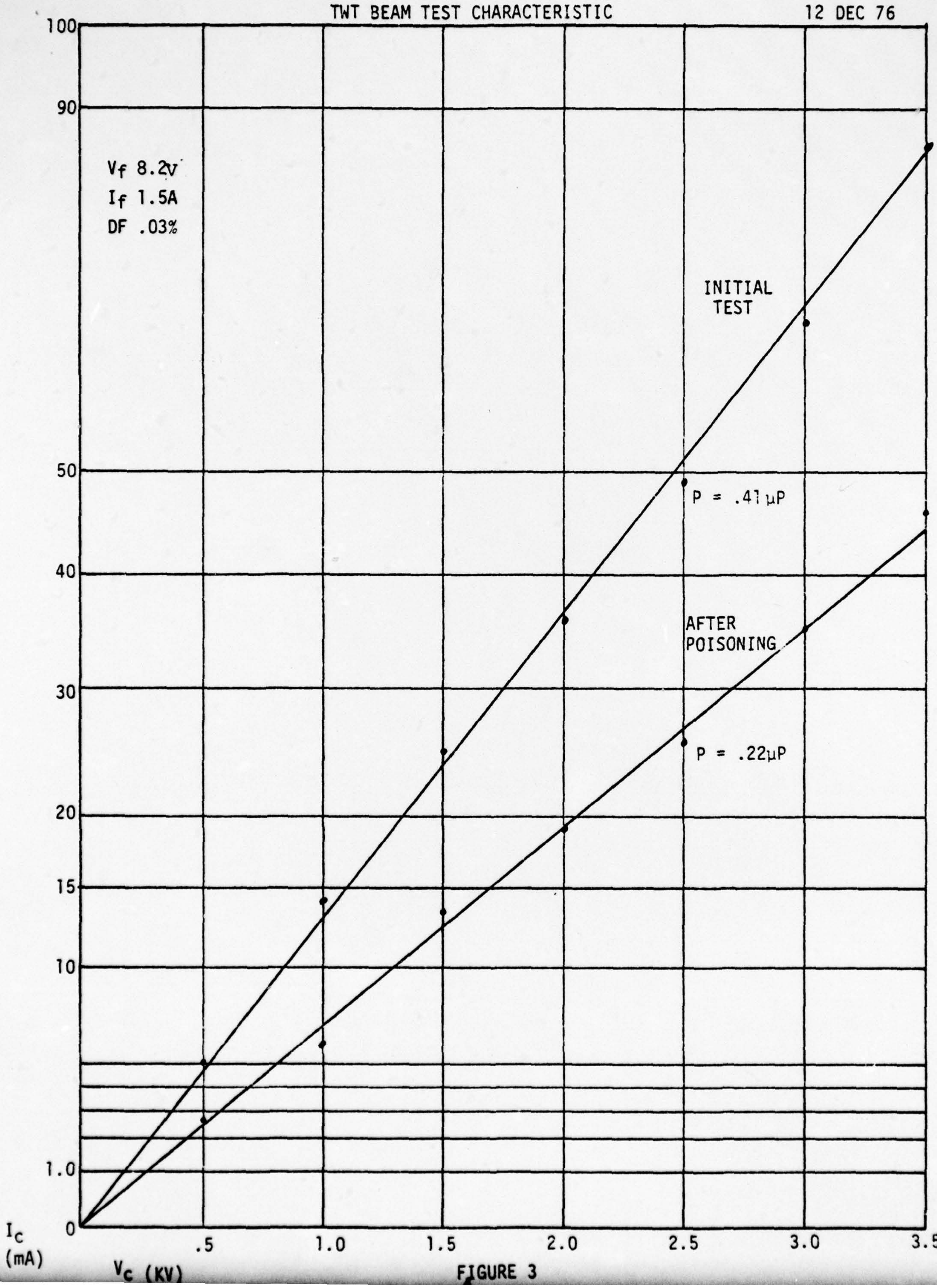
TWT BEAM TEST CHARACTERISTIC
12 DEC 76
Vf 8.2V
If 1.5A
DF .03%
INITIAL TEST
P = .41µP
AFTER POISONING
P = .22µP
100
90
50
40
30
20
15
10
1.0
0
Ic (mA)
.5
1.0
1.5
2.0
2.5
3.0
3.5
Vc (KV)

FIGURE 3

and the vacuum measured at the header of the beam tester improved from 10^{-6} to 2.10^{-8}. The impregnated cathode was replaced by the Medicus cathode. Figure 4 shows that the $I^{2/3}$-V characteristic is never a straight line. However the Medicus cathode was more stable in operation than the impregnated cathode.

1.4 Beam Tester

During this period of the program, experimental results were obtained with the miniature beam tester.

A probe assembly consisting of 5 probe wires and a collector shield as schematically shown in Figure 5 was mounted onto the rotating shaft and inserted into the beam tester. During assembly, the melted bead of probe wire No. 5 broke off, so that the data collected with this probe must be used very carefully and may be doubtful. The current collected by each individual probe was measured by rotating the probe assembly $\pm 180^{\circ}$ from a reference position at different z-positions in the barrel, simulating the interaction space. The different z-positions, numbered 0, 1, ...15, are schematically shown in Figure 6. The distance between position n and n + 1 was measured to be .100 inches. The pitch of the magnet field can be assumed to be 1.08 cm (.432 inches).

Figure 7 shows the typical current distributions as measured as a function of ϕ for different z-positions (0, 2, 4, 6, 8, 10). From these curves, the following conclusions can be drawn:

1. The current distribution is independent on ϕ at the z-position of 2. Here, the current is "homogeneously" distributed.

2. A second "homogeneous" current distribution occurs at a position z located between 8 and 10 (in fact, it is closer to 8 than to 9).

3. The distribution for other z-positions exhibits maxima and minima. The maxima of a given curve (probe) are not equal, and as such the beam must exhibit a complex variation with the distance R from the center.

Points 1 and 2 seem to indicate that the beam exhibits a periodicity with z, the wavelength (half the wavelength!) being equal to about .650", or about 1.5 times the periodicity of the magnetic field. This behavior can be understood in view of Figure 17 of reference*, which shows that such a periodicity occurs if the beam is injected with a tilt angle of a few degrees.

Point 3 above is substantiated by Figure 8, which shows a picture of the beam collector after removal from the beam tester. Clearly visible is a ring of high erosion, located approximately as shown in Figure 9. The autopsy reveals that this ring is off center by about 1.6 mils. This indicates that the beam seems to be hollow in the interaction space.

* O. Doehler, R.R. Moats, Low Cost Expendable TWT Amplifier for ECM, Final Report, Contract No. N00173-75-C-0464, 1976.

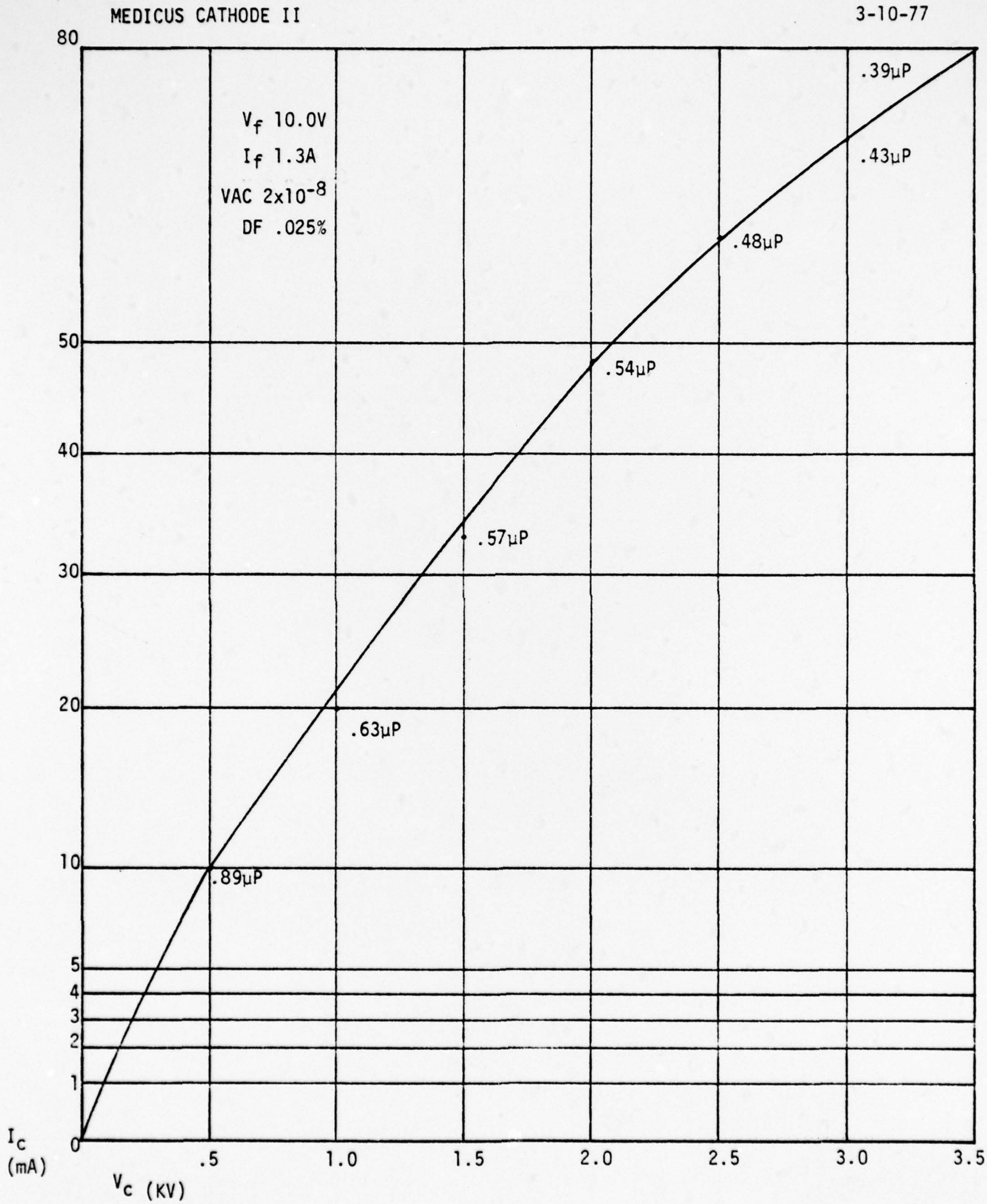

FIGURE 4: TWT BEAM TESTER CHARACTERISTIC

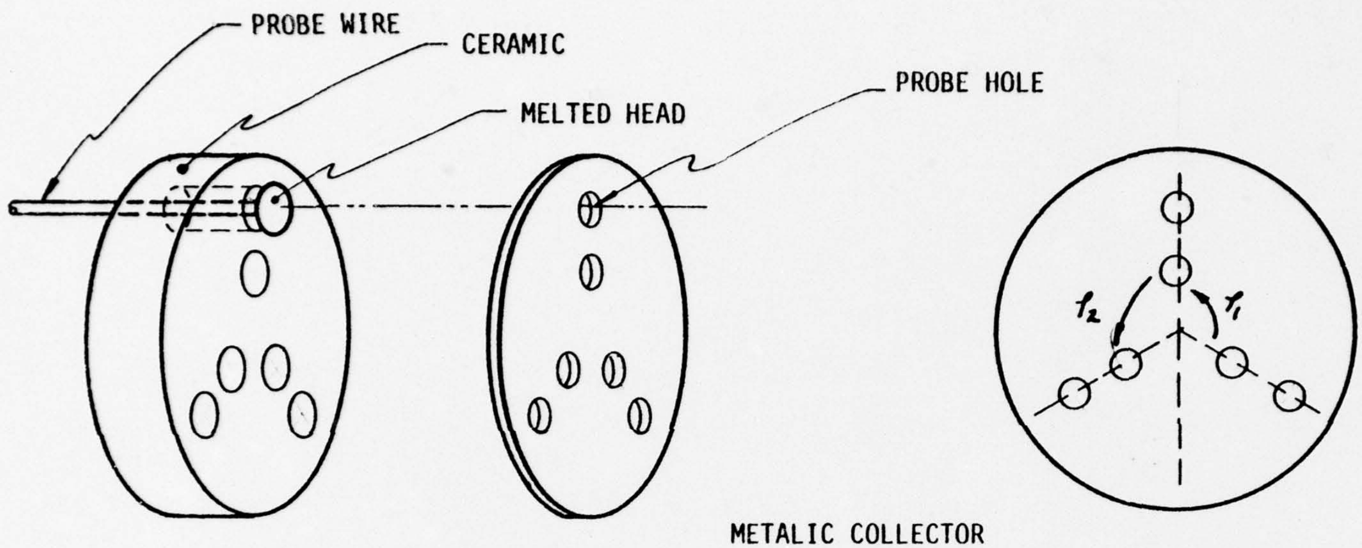

FIGURE 5: SCHEMATIC OF THE PROBE ASSEMBLY

COORDINATES OF PROBE HOLES IN COLLECTOR: $\rho_1 = 23$; $\rho_2 = 7$; $\rho_3 = 17.5$; $\rho_4 = 12.6$; $\rho_5 = 2.5$; $\phi_1 = 120°$; $\phi_2 = 120°$

DIAMETER OF PROBE HOLES: 5 (ALL DIMENSIONS IN MILS [1/1000 INCHES])

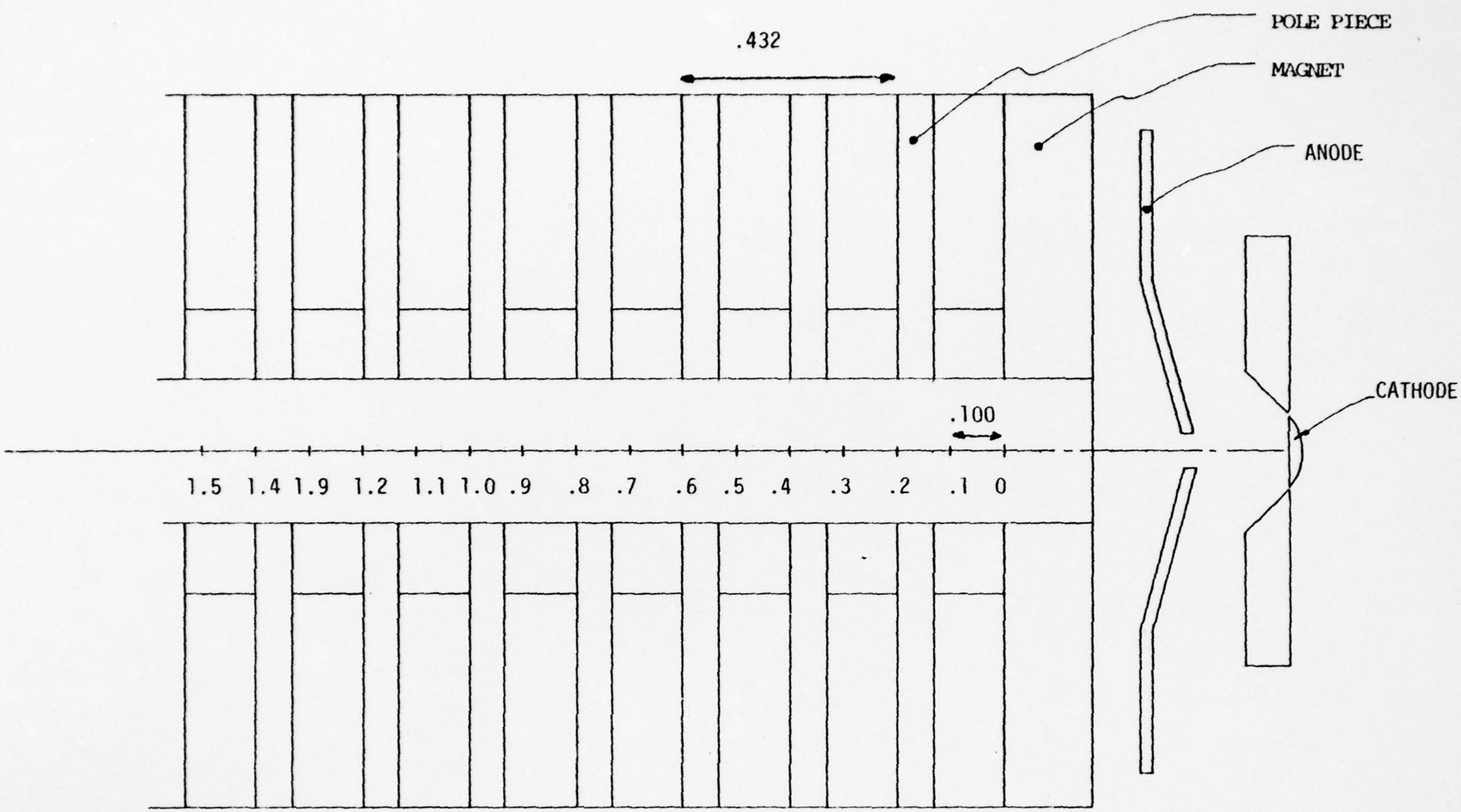

FIGURE 6 : DIFFERENT Z-POSITIONS

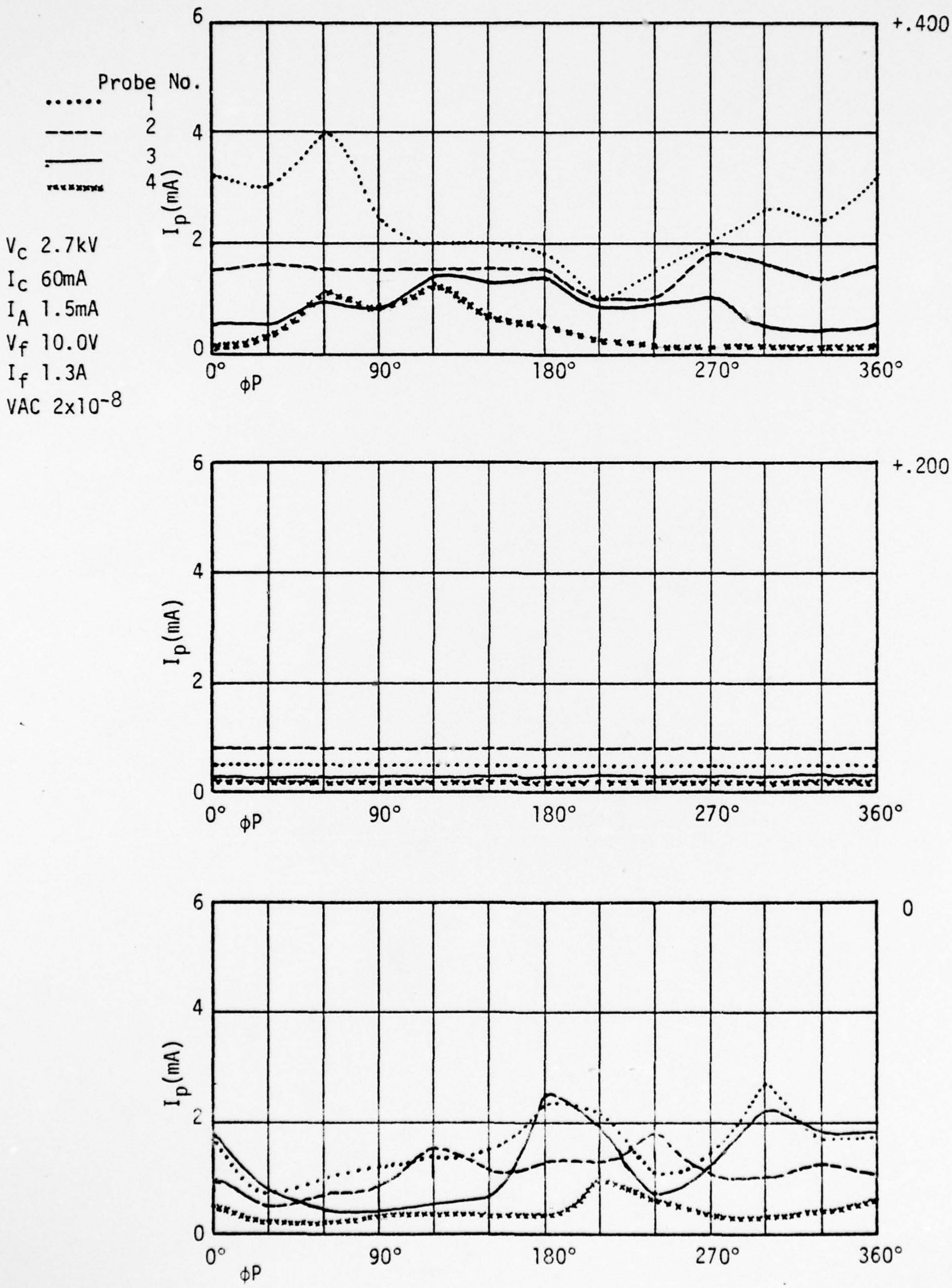

FIGURE 7A: CURRENT DISTRIBUTION (Z = 0, .2, .4)

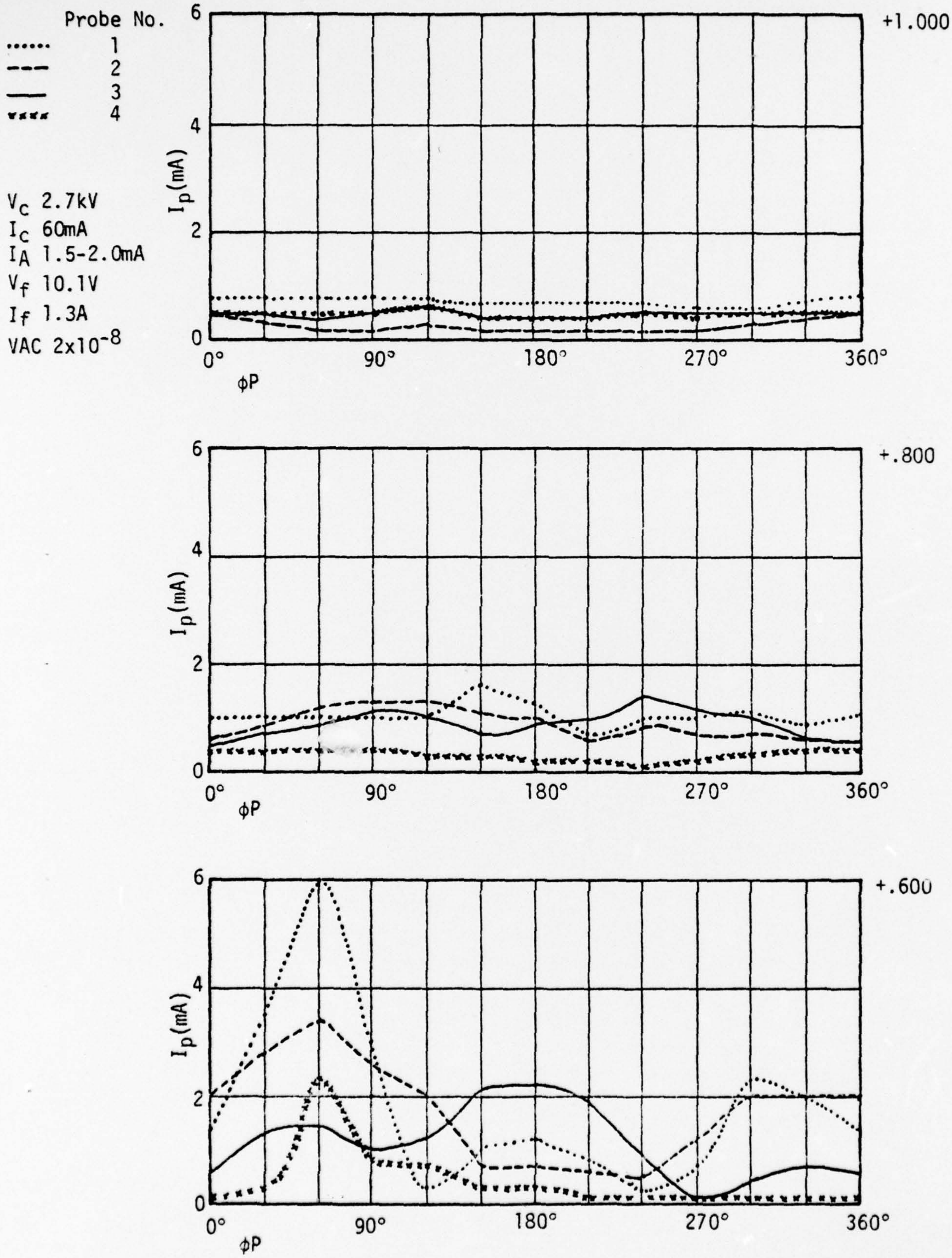

FIGURE 7B: CURRENT DISTRIBUTION (Z = .6, .8, 1.0)

Figure 8: Picture of the beam collector showing the location of the probe holes and the ring of high erosion around the center of the collector.

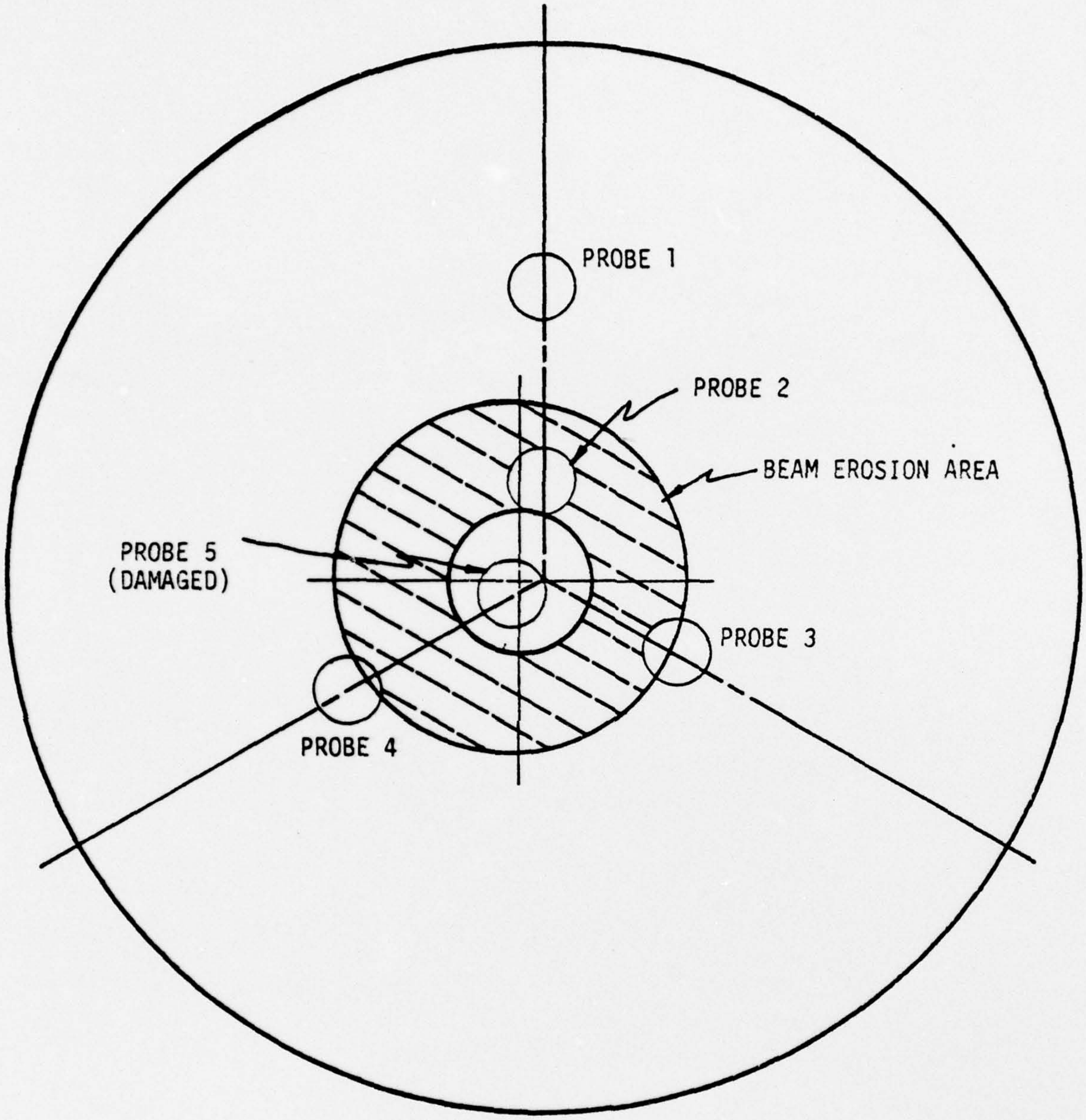

FIGURE 9: GEOMETRY OF THE RING OF HIGH EROSION ON THE COLLECTOR PLATE

A more quantitative evaluation of the experimental results obtained has been initiated and will be discussed in the following.

Let us assume that the beam is isotropic with respect to its own center i.e., the current distribution i (R,ψ) will then be given by:

$$I = \int dF\, i(R) \qquad (1)$$

and will neither depend on the angle ψ , since both F and i are independent of ψ. Therefore the total current collected will only depend on the relative distance R between the probe center P and the beam center 0'.

If the center 0 of the probe assembly is displaced from the beam center 0', (see Figure 10) then the vector R is given by:

$$\vec{R} = \vec{\rho} - \vec{Y}_o$$

and as such, the current will only depend on

$$I = I(R) = I\left([\rho^2 + Y_o^2 - 2\rho Y_o \cos(\phi - \phi_o)]^{\frac{1}{2}}\right) \qquad (2)$$

where (ϕ_o, Y_o) describe the relative position of the beam center with respect to the center.

Consequently, at each position z, the current distribution of each probe as measured as a function of the angle ϕ

$$I^{(i)} = \sum^{N} (A_n^{(i)} \sin n\phi + B_n^{(i)} \cos n\phi) \qquad (3)$$

where the index i refers to the i-th probe, must have the following form:

$$I^{(i)} = \sum^{N} C_n^{(i)} \cos n(\phi - \phi_o^{(i)}) \qquad (4)$$

where $\phi_o^{(i)}$ represents the initial angle between the probe i and the center 0' of the beam, and where the difference $\phi_o^{(i)} - \phi_o^{(j)}$ represents the angle between the probes i and j as measured on the beam collector shield (+120°). As an example, let us consider the current distribution measured at the z-position No. 6. for probe No. 1. Using the Fourier series:

$$I = \sum_{o}^{5} (A_n \sin n\phi + B_n \cos n\phi) = \sum_{o}^{5} C_n \cos n(\phi - \phi_o)$$

one obtains by using the least square approximation the results shown in Table 3. Since ϕ was varied by 30° increments, the Fourier approximation was made up to N=5, corresponding to 11 unknown coefficients A_n, B_n. As a result, and average value $\phi_o \simeq 57° \pm 5°$ is obtained. A similar analysis for probe number 2 at the same z-position leads to $\phi_o \simeq 55° \pm 7°$. Note that probe 1 and 2 on Figure 5 do have the same reference angle position.

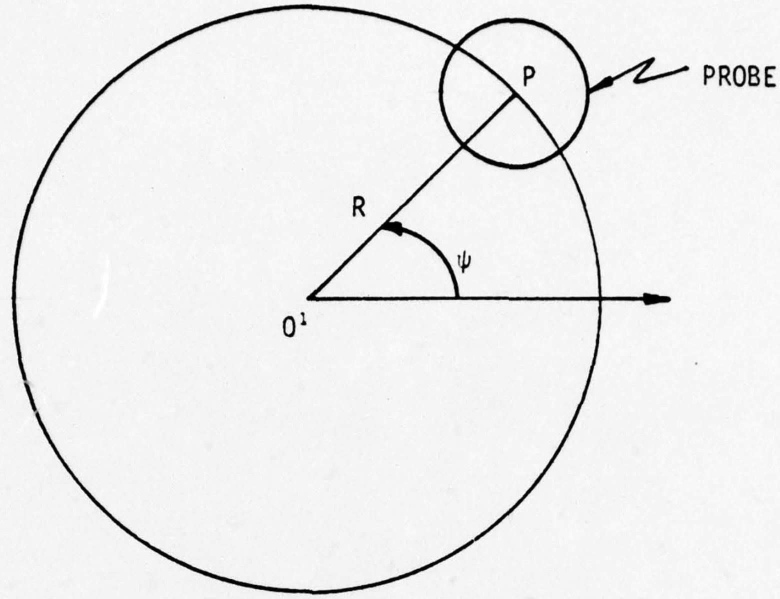

O^1: BEAM CENTER

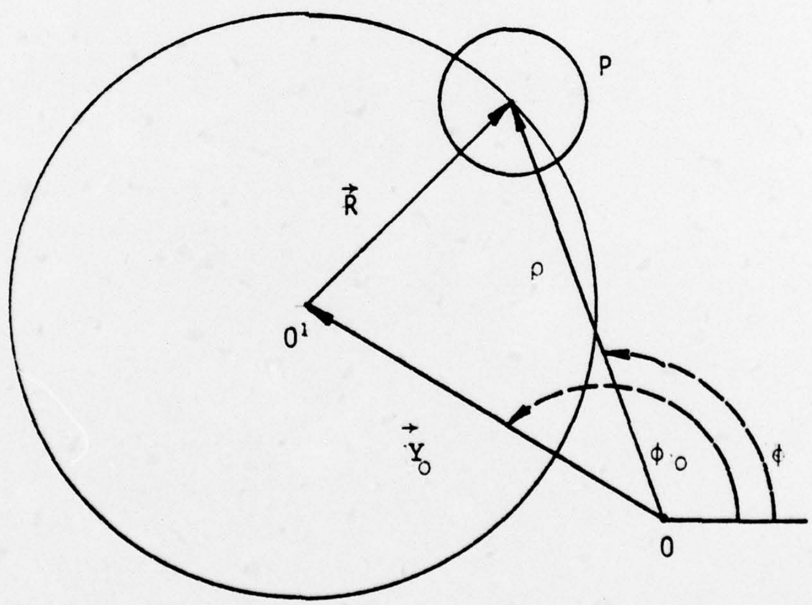

O: CENTER OF PROBE ASSEMBLY

FIGURE 10: BEAM AND PROBE COORDINATES

TABLE 3

n	0	1	2	3	4	5
A_n	-	1.10	.74	-.94	-.36	-.05
B_n	1.9	1.23	.40	-1.40	-.38	.17
C_n	1.9	1.65	.83	1.41	.52	.17
$n\phi_o$	-	42°	118°	183°	223°	-17°
ϕ_o	-	42°	59°	61°	55°	68°

Fourier Approximation (probe 1, Z=6). (For n=5, 360° were added to obtain $\phi_o = 68°$).

For probe No. 3, one obtains $\phi_o^{(3)} \simeq 164°$, while probe No. 4 leads to $\phi^{(4)} = 66°$. While the differences $\phi_o^{(1)} - \phi_o^{(2)} = 2°$; $\phi_o^{(2)} - \phi_o^{(3)} = 109°$ should be 0 and 120° from the geometry of the probes, the difference $\phi_o^{(4)} - \phi_o^{(1)}$ should also be 120°. The reason why this does not occur is not known at this point.

Figure 11 shows the values of $\phi^{(i)}$ as a function of z-position, where $\phi^{(i)}$ was obtained as discussed above. For probes 1 and 2, as well as for probes 3 and 4, the angle of rotation first decreases, passes through a minimum, and increases again. The curves corresponding to probes 1 and 2 are similar to within experimental errors. Probe No. 3 is shifted by 120°, as it should be, while the small shift of probe No. 4 is not understood (it should be -120° or +240°). The autopsy has revealed that the melted wire head of probe wire 4 was not located properly under the corresponding collector hole.

As a first result, therefore, it seems that the beam center (guiding center) rotates in a rocking motion around the geometric axis of the magnetic field. This is understandable in the following way. As the beam passes through the first magnet (z = 0, 1), it "sees" a given direction of magnetic field and thus rotates in a direction which reduces ϕ_o. At position z = 2, the beam has entered a region in which the magnetic field is reversed and the beam will feel a deceleration until it enters magnet No. 3 (z = 4), where it "feel" an accelerating magnetic field. This results in a rocking motion of the guiding center.

1.5 PPM Focusing

1.5.1 Ferrite magnets

It was reported (first trimestrial report) that the ferrite magnets had much stronger thermal reversible and irreversible effects than claimed by the supplier. A stack of 20 magnet periods were mounted and thermal cycled.

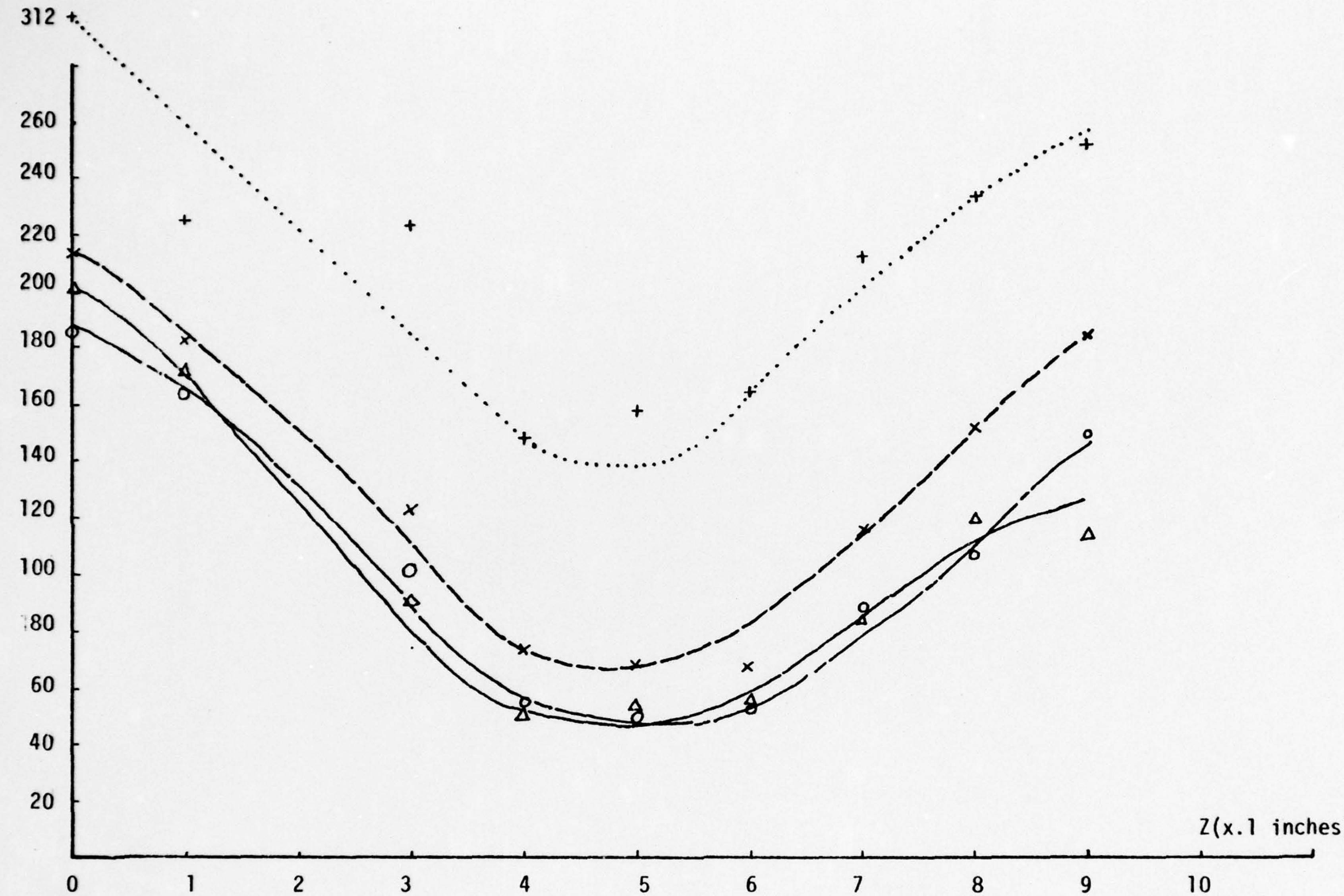

FIGURE 11: ROTATION ANGLES $\phi_o^{(i)}$ AS A FUNCTION OF Z

In the first run, the bare magnets were stabilized at 250 gauss by Indiana gereral, and in the second run the same magnets were stabilized at 170 gauss. This magnetic field was the lowest field measured in the first run. Table 4 shows the experimental results, which indicate, that the irreversible effects are much too high even for the lower stabilized field to meet the criteria for the maximum tolerable random field variation. This means that ferrite magnets cannot be used in a low cost TWT submitted to thermal cycling down to -50°C.

1.5.2 Alnico:

Alnico 8 magnets were purchased from Indiana General. The bare magnets were stabilized at 250 gauss and submitted to assembly, deassembly, and thermal cycling. Table 5 shows the results. Stabilized Alnico 8 can be used in the low cost TWT, the standard deviation is approximately equal to the upper limit for the tolerable random peak magnetic field variation. (See first trimestrial report)

1.5.3 Samarium - Cobalt

A stack of 5 samarium-cobalt magnets were made available to Northrop by D. Zavadil of M.E.C. Table 6 shows the experimental results.

The reversible thermal drift is higher than the published data in the literature. However with the new temperature compensating rare earth cobalt with doping by gadolinium, the thermal drift can be easily tolerated.

The measured crossed fields can be accepted, if the calculation presented in the first final report are correct.

1.6 "T" Shape Helix

The first "T" shape helixes were constructed on a lathe and wound on a bare mandrel, covered with aquadag. The helix on the mandrel after annealing were inserted into a high precision glass and the helix fixed by shrinkage of the glass.

Figure 12 shows the v/c vs frequency of two helixes constructed in the same manner. The first helix had a stronger shrinkage and the dielectric loading factor is much lower, indicating, that the distance between the outer diameter of the helix and the inner diameter of the dielectric barrel is critical.

Figure 13 and 14 shows the coupling impedance measured by the phase shift variation between the input and the output by moving an Al_2O_3 rod inside the helix.

TABLE 4

IRREVERSIBLE EFFECTS OF FERRITES

		STANDARD DEVIATION
I.	BARE MAGNETS STABILIZED AT 250 GAUSS	.6%
	STACK	4.3%
	AFTER - 40°C	7.8%
	AFTER - 50°C	7.8%
	AFTER - 50°C 2nd	8.0%
	BARE MAGNETS AFTER CYCLING	9.7%
II.	BARE MAGNETS STABILIZED AT 170 GAUSS	.75%
	STACK	2.2%
	AFTER - 20°C	2.4%
	AFTER - 40°C	2.5%

REVERSIBLE EFFECTS OF FERRITES

$\frac{\Delta B}{B} / {}^{\circ}C$	.191 - .283/°C

TABLE 5

ALNICO 8 STACK

	STANDARD DEVIATION
BARE MAGNETS STABILIZED AT 250 GAUSS	.54%
BARE MAGNETS AFTER ASSEMBLING AND DEASSEMBLING	.92%
STACK	1.22%
AFTER CYCLING	1.22%
BARE MAGNETS AFTER CYCLING	1.26%
AFTER 2nd CYCLING BARE MAGNETS	1.16%

TABLE 6

SAMARIUM-COBALT

NO IRREVERSIBLE EFFECTS BETWEEN	-55°C to +100°C
THERMAL DRIFT	.062 to 0.095% /°C
CROSSED FIELD	.35 to 0.6%

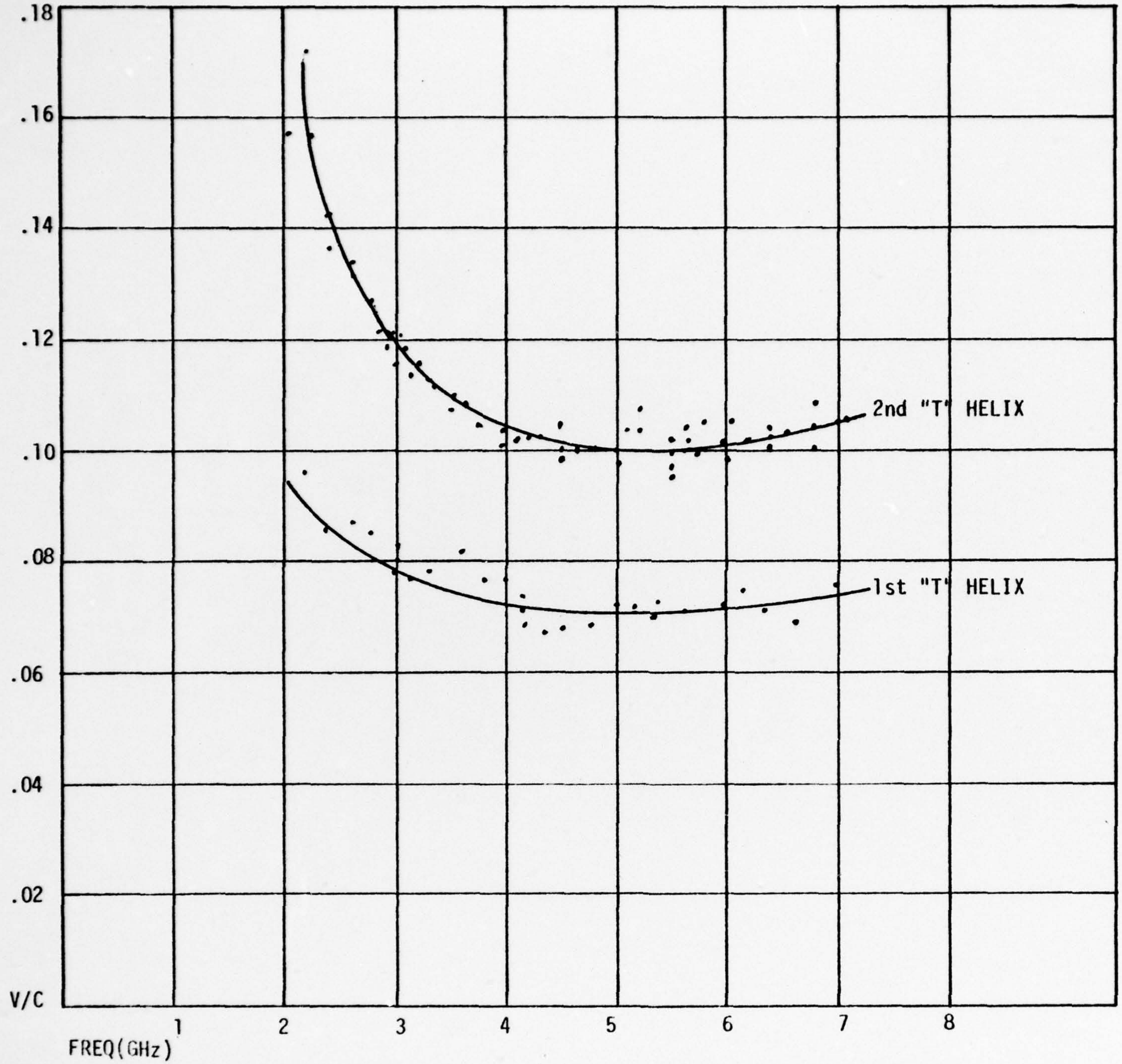

DISPERSION CURVE V/C vs. FREQUENCY

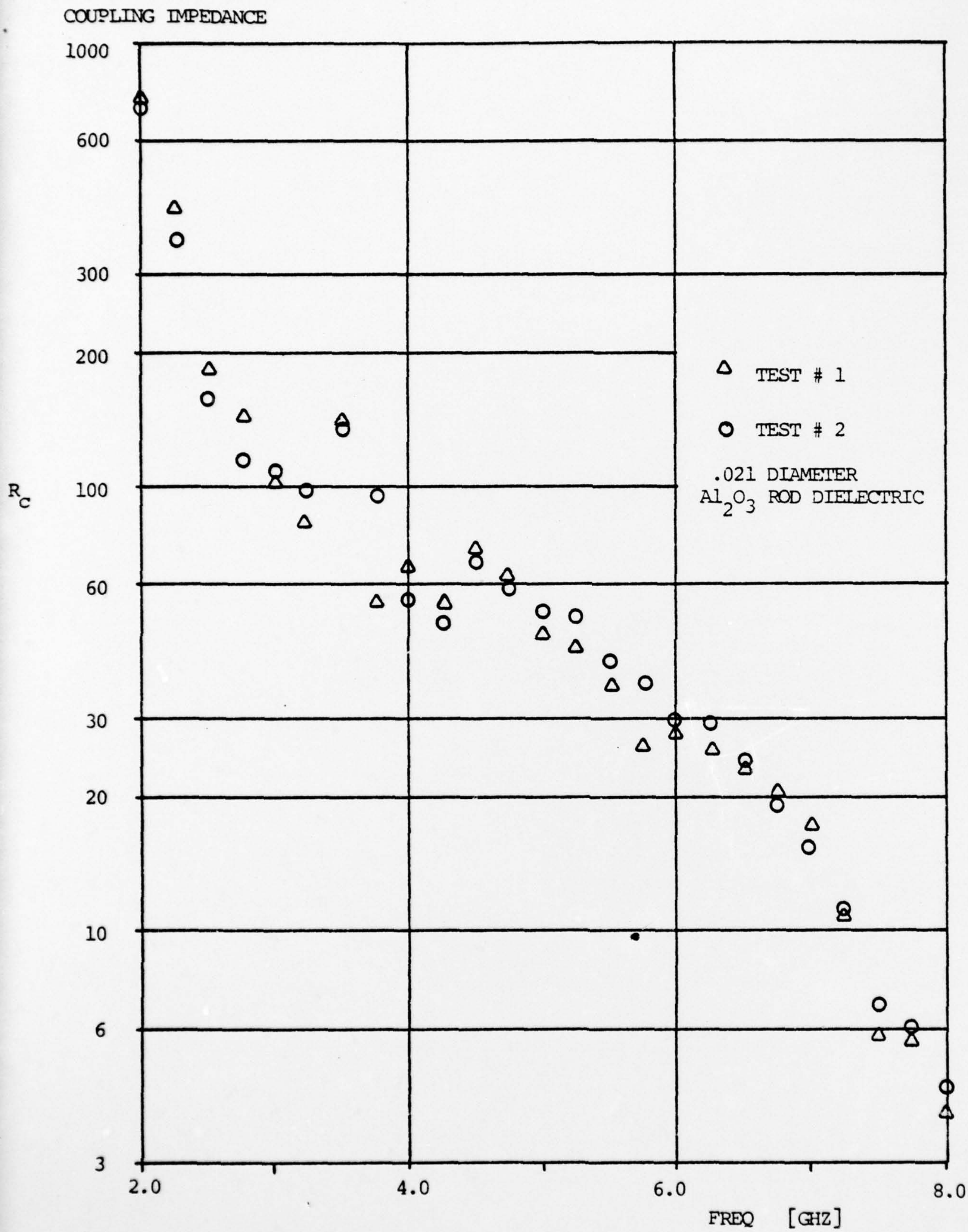

FIGURE 13 COUPLING IMPEDANCE OF 'T' SHAPE HELIX

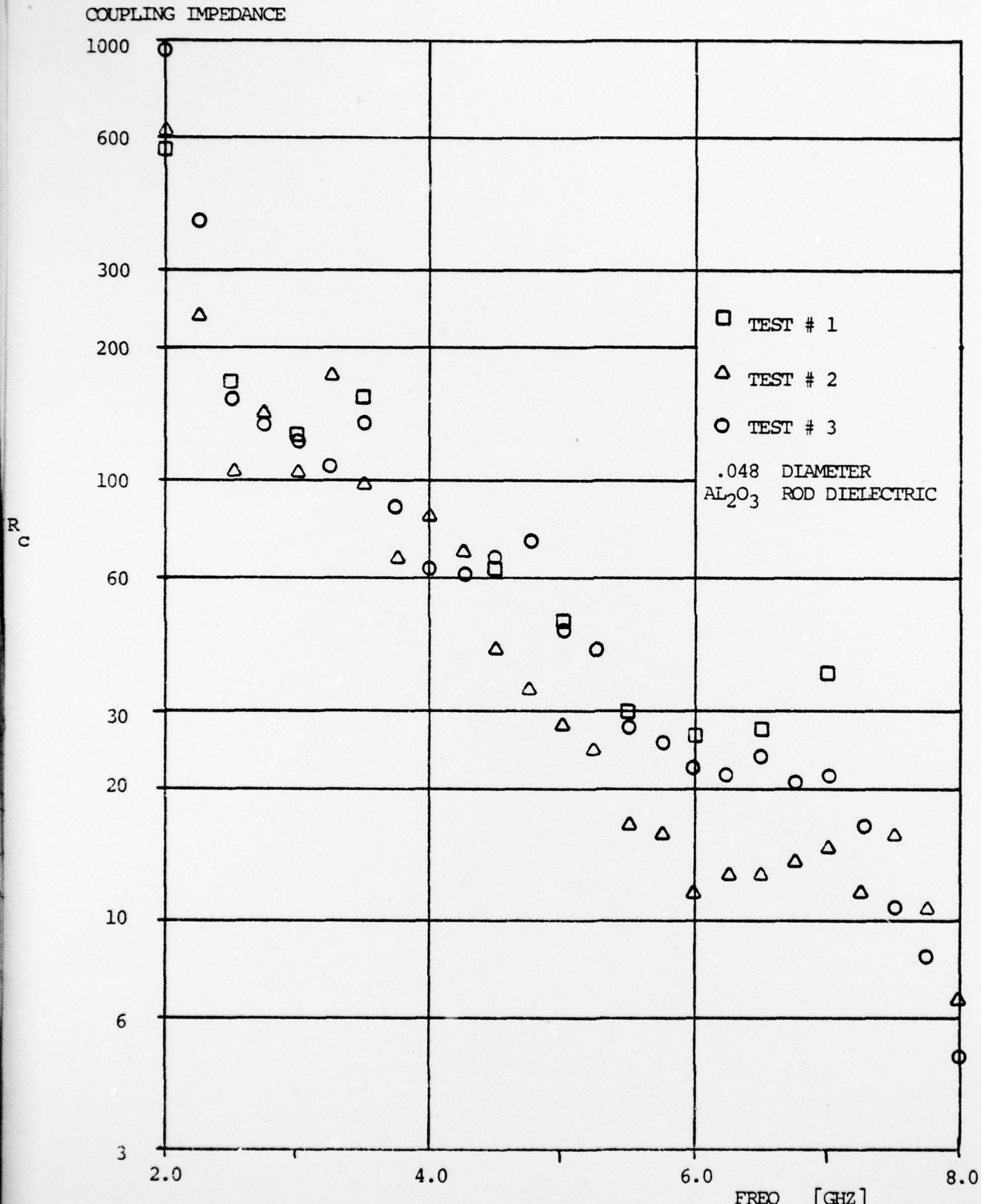

FIGURE 14 COUPLING IMPEDANCE OF 'T' SHAPE HELIX

The inner diameter of the helix was 2.15 mm. The two dielectric rods had a diameter of .52 mm (figure 13)and 1.22 mm (Figure 14) respectively.

A relation between phase shift and coupling impedance was used which was derived in a final report of N.R.L.* This relation is equivalent to an equative used at N.R.L.**

The precision of the measurements is not high, because the regularity of the line is poor. However the coupling impedance is relatively high. For a $\gamma a = 1.5$ equivalent to 6.6 GHz the coupling impedance is still larger than 10 Ω (measured with the rod of 1.22 min and of 20 Ω (measured with the rod of .52 min.) (Note that the thinner rod introduces less perturbation which corresponds to higher accuracy).

* Final report: Feasibility study on a multiple Helix Traveling Wave Circiut - X - Band. N.R.L. N00014-71-C-0168. 1-26-1971

** H. Arnett: Private communication

2. PROBLEMS:

1. The main problem encountered was the poisoning of the cathode of the beam tester so that only a few measurements could be made.

2. It is difficult to obtain in time the wire for the "T" shape helix.

3. The precision of the "T" shape helix is insufficient.

4. The gun design is not reliable.

3. PROPOSED WORK IN THE NEXT TRIMESTER

3.1 Construct a new more reliable gun.

3.2 Improve the precision and reliability of the "T" shape helix.

3.3 Start input and output coupler design, which has not been done in the second trimester.